JOURNAL OF MATERIALS SCIENCE **32** (1997) 6567–6572

Interfacial reaction and adhesion between SiC and thin sputtered nickel films

C. S. LIM*, H. NICKEL, A. NAOUMIDIS**, E. GYARMATI
Institute for Materials in Energy Systems, Research Center Jülich, D-52425 Jülich, Germany

Thin sputtered nickel films grown on SiC were annealed in an Ar/4 vol% H_2 atmosphere at temperatures between 550 to 1450 °C for various times. The reactivity and the reaction-product morphology were characterized using optical microscopy, surface profilometry, X-ray diffraction, scanning electron microscopy and electron probe microanalysis. The reaction with the formation of silicides and carbon was observed to first occur above 650 °C. Above 750 °C, as the reaction proceeded, the initially formed Ni_3Si_2 layer was converted to Ni_2Si and carbon precipitates were observed within this zone. The thin nickel film reacted completely with SiC after annealing at 950 °C for 2 h. The thermodynamically stable Ni_2Si is the only observed silicide in the reaction zone up to 1050 °C. Above 1250 °C, carbon precipitated preferentially on the outer surface of the reaction zone and crystallized as graphite. The relative adhesive strength of the reaction layers was qualitatively compared using the scratch test method. At temperatures between 850 to 1050 °C the relatively higher critical load values of 20–33 N for SiC/Ni couples are formed.

1. Introduction

The study of ceramic–metal interfacial reactions is of great interest in materials science because of the technological applications of devices fabricated from both ceramic and metal components. SiC is used not only for high-temperature applications in the form of a monolithic ceramic or in ceramics or metal–matrix composites [1–3], but also as a semiconducting material for high-temperature, high-frequency and high-power electronic devices [4–6]. For both these application areas, as well as for the process of SiC-SiC and SiC-metal joining with metallic intermediates, a detailed knowledge about SiC/metal interactions and the thermal stability of SiC/metal interfaces is of primary importance [7–9]. The chemical, thermal and crystallographic compatibility, which is dependent on the interfacial reaction, thermal expansion mismatch and lattice mismatch, must be considered to establish the thermal stress gradients across the reaction zone.

The interaction between the SiC and a metal during thermal annealing determines the properties of the contacts. One area of interest is the use of metals forming silicides on SiC substrates at low temperature, in the attempt to form contacts with thermal annealing. Many metals have a strong tendency to interdiffuse at semiconductor–metal interfaces and most metals readily form carbides or silicides. A thorough characterization and understanding of SiC–metal interfaces, in terms of reactivity and thermal stability, is therefore crucial in the design of SiC devices. Several studies have been reported in the literature which allow a basic understanding of the physical and chemical interactions at the SiC–metal interfaces [10–17]. Depending on the experimental conditions the interaction of SiC with different metals has resulted in the observation of different silicides, free carbon, metallic alloys and carbides as reaction products.

Cobalt and nickel provided good high-temperature contacts with SiC. They are also of specific interest due to their silicide-forming tendency at low temperature, making them suitable for metallization. In previous studies [18, 19], the interaction between SiC and thin sputtered cobalt films and foils in the temperature range 500–1250 °C were reported. At present only a few detailed studies on the interaction of thin films with SiC at low temperatures have been reported in the literature [20–25]. The aim of this paper is the study of the interfacial reaction and adhesion of thin (2 μm), sputtered Ni films deposited on SiC. In particular we aim to identify all the reaction products in the diffusion zone by means of X-ray diffraction (XRD), and also study the morphology of the formed scale in the temperature range 550–1450 °C. The adhesion of the formed interface between the polycrystalline SiC and the thin nickel layers is discussed on the basis of measurements of the critical load, using the scratch test. Furthermore, a thermodynamic argument is proposed to interpret the interactions in the SiC/Ni system.

* *Present address*: Ceramic Materials Research Institute, Hanyang University, Seoul 133-791, Korea
** Author to whom correspondence should be addressed.

0022–2461 © *1997 Chapman & Hall*

2. Experimental procedure

The materials used for the experiments, the sputtering technique, the annealing conditions, as well as the characterization procedure have been previously described [18]. Highly dense sintered α-SiC samples with a thin sputtered nickel film were placed in a furnace that was evacuated to 6×10^{-4} Pa and subsequently filled with a gas mixture of Ar/4 vol % H_2. Annealing in the temperature range of 550–1450 °C occurred for 0.5–2 h. The heating rate was set between 20 and 30 K min^{-1} and the cooling rate between 5 and 10 K min^{-1}.

The surface of the samples were characterized by surface profilometry and optical microscopy. The identification of the reaction products to allow the qualitative extent of the reaction between the SiC and the thin sputtered nickel films to be estimated was performed by determining the phase fractions from relative XRD peak intensities of at least three coincidence-free reflections. The reaction sample couples were cut using a diamond saw and then embedded in copper resin. After mounting they were ground on a diamond disc, polished with diamond pastes of grade 30, 15, 6, 3 and 1 μm. The polished cross-sections were characterized using scanning electron microscopy (SEM) and electron probe microanalysis (EPMA).

The adhesive strength is presented in terms of the critical load determined by the scratch test method. A commercially available scratch test apparatus, designed by the Laboratoire Suisse de Recherches Horlogères (LSRH), was used to study the adhesion of the thin sputtered nickel film on the SiC substrate before and after various annealings. The unit has a diamond stylus in the form of a Rockwell C 120° cone with a spherical tip radius of 200 μm. Loads were applied continuously in steps of 1 N up to a maximum of 200 N. The scratch equipment was fitted with an acoustic signal detector in the form of an accelerometer mounted just above the diamond stylus. It registered signals emitted in the range 0–200 mV. Samples mounted on to a slide dish were scratched with a standard scratch speed of 10 mm min^{-1}. The voltage output signal was recorded in order to determine whether a correlation could be established between the signal, the scratch characteristics and the loss of coating adhesion. At low loads the curves are smooth. When coating loss occurs, the signal increases suddenly. The measured acoustic emissions were compared with the microscopy observations of the tracks formed by the stylus.

3. Results

3.1. Surface morphology

Fig. 1 is an SEM micrograph of a typical as-sputtered surface of a nickel film on a SiC substrate. The coating has a porous columnar microstructure (zone-1 according to Thornton's structure model) that is consistent with low adatom mobility. According to an XRD analysis, the deposited nickel film crystallized in the cubic modification. Fig. 2 shows the thickness measured for the sputtered nickel and cobalt [18] films as a function of sputtering time. The growth rate of the nickel films was calculated to be 66.7 nm min^{-1}, which is much higher than the rate for cobalt (11.7 nm min^{-1}) under the conditions used (magnetron sputtering system, d.c. potential 400–500 V, partial pressure of Ar 4.0 and 7.0 Pa, respectively). The relative sputtering yields of cobalt and nickel in an argon sputtering gas energy of 500 eV are 1.22 and 1.45 atoms per ion respectively [26]. The efficiency of sputtering for nickel is higher than that for cobalt at the same sputtering gas energy. In our sputtering process a bias voltage was used during the nickel deposition but this was not the case for the cobalt growth. This resulted in a thinner, denser coating of nickel due to enhanced adatom mobility.

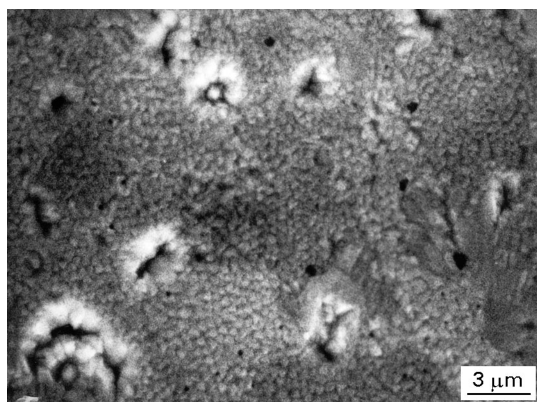

Figure 1 Scanning electron micrograph of the surface structure of the nickel film (2 μm thick) deposited on the SiC substrate.

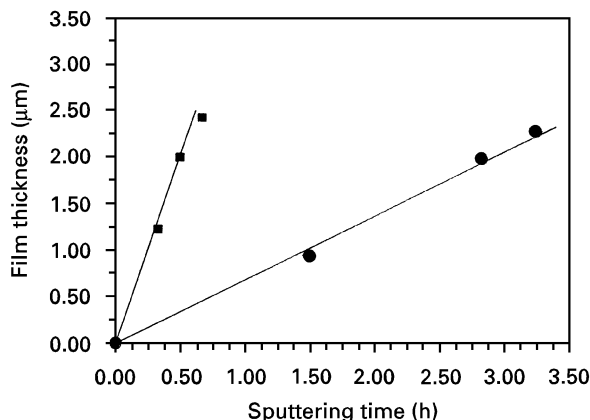

Figure 2 The thickness of the nickel thin films compared with cobalt thin films as a function of sputtering times. The growth rates of the nickel and cobalt films in a magnetron-type d.c. sputtering source were determined to be 66.7 and 11.7 nm min^{-1} respectively. The growth conditions for the nickel film were: As argon partial pressure 7.0 Pa, d.c. potential 0.4 kV, bias voltage − 150 V, with the cathode being the magnetron. The conditions for the cobalt were argon partial pressure 4.0 Pa, d.c. potential 0.5 kV, with the cathode being the magnetron.

Annealing experiments were performed in the temperature range of 550–1450 °C. In most cases, thin metal films were well coupled with the ceramic after annealing at temperatures between 650 to 1250 °C. A reaction product was first detected at 650 °C (after 2 h). Photographs of the surface of the reaction couples of SiC/Ni after annealing at 650, 950, 1050 and 1250 °C are shown in Fig. 3(a–d). After annealing at

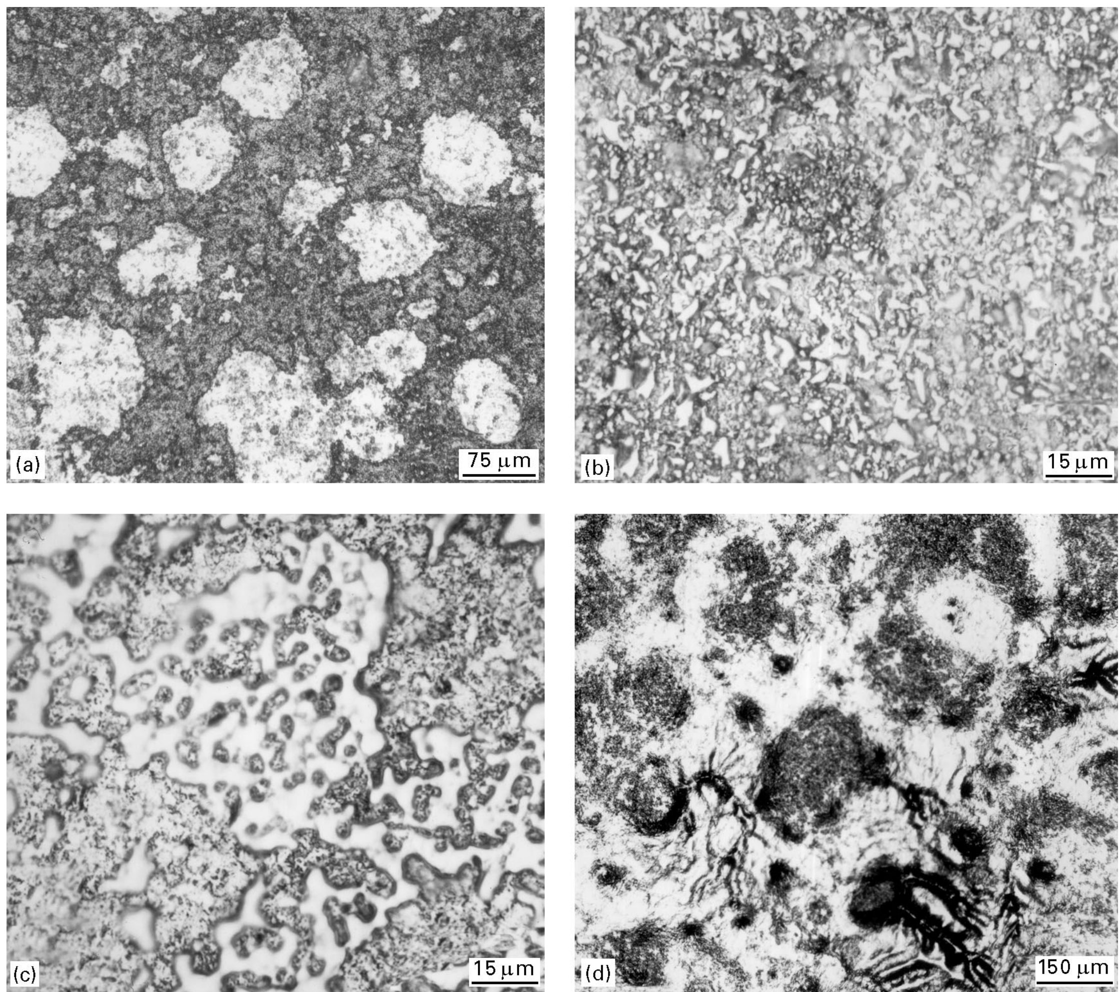

Figure 3 Surface structures of the reaction couples of SiC/Ni after annealing at (a) 650 °C for 2 h, (b) 950 °C for 2 h, (c) 1050 °C for 2 h and (d) 1250 °C for 2 h. The thickness of the nickel film on the SiC substrate was fixed at 2 μm.

650 °C (Fig. 3a), shadow contrasts on the surface were observed. A fine agglomeration of the reaction products was observed after annealing at 950 °C for 2 h (Fig. 3b). Annealing at 1050 °C for 2 h, resulted in a surface morphology that showed relatively increased agglomerations with partial melting (Fig. 3c). After annealing at 1250 °C, severe reactions were observed among the randomly distributed precipitations on the surface (Fig. 3d). The XRD analysis of this sample identified the formation of graphite. The extent of the reaction was indicated by the measurement of surface roughness with a surface profilometer. The average roughness of the annealed surface increased with an increase in the annealing temperature.

3.2. Reaction products

The identification of reaction products was confirmed by determining the relative XRD peak intensities. Fig. 4 shows the qualitative phase analysis of the SiC/Ni reaction couples based on the XRD analysis for different temperatures and times. Below 650 °C, no reaction was observed. At 650 °C most of the nickel layer reacted and formed the silicides Ni_2Si and Ni_3Si_2. Unreacted nickel was crystallized, as identified by XRD, after this heat treatment as the cubic modification. It was distributed predominantly in the film surface, no carbide formation, either Ni_2C or Ni_3C, was detected by the XRD. At this temperature we could not find a layered structure of Ni_2Si and Ni_3Si_2 because of the very thin reaction thickness.

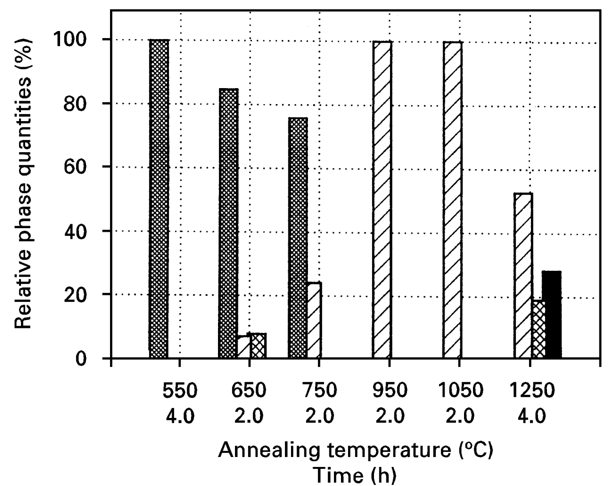

Figure 4 Quantitative analysis of the SiC/Ni reaction couples based on relative XRD phase estimation for various annealing conditions. Key (■) Graphite, (⊠) Ni_3Si_2, (▨) Ni_2Si and (▩) Ni.

At 750 °C the Ni_3Si_2 phase was transformed into the Ni_2Si phase. Depending on the annealing time, the

relative quantities of Ni_2Si increased while the Ni_3Si_2 phase content decreased simultaneously. At 750 °C the Ni_3Si_2 was fully consumed after 2 h. At 950 °C the entire nickel film was fully converted to Ni_2Si after 2 h. This phase is the only observed silicide in the reaction zone up to 1050 °C. After 2 h at 1250 °C, the Ni_2Si phase along with small quantities of Ni_3Si_2 and graphite was detected. Graphite is presumably developed by graphitization of carbon formed through the reactions $Ni + 1/2SiC = 1/2Ni_2Si + 1/2C$ and $Ni + 2/3SiC = 1/3Ni_3Si_2 + 2/3C$. The reason why the Ni_3Si_2 phase was formed at 1250 °C may be attributed to the fully consumed nickel and the predominant diffusion of silicon in the reaction zone.

A cross-section of the annealed samples treated at 950 °C for 2 h was qualitatively analysed by EPMA. Fig. 5 shows the line scan of the X-ray intensity for the elements nickel, silicon and carbon across the reaction zone. The corresponding phase distribution is noted on this diagram. Over the interface, a mixture of Ni_2Si with carbon was identified. The line scan indicates that a periodic maximum of carbon intensity corresponds to the minimum of the nickel intensity. A cross-sectional scanning electron micrograph (Fig. 6) shows the reaction zone after annealing at 1050 °C for 2 h. In the region neighbouring the SiC, a two-phase mixture consisting probably of Ni_2Si (as identified by XRD) with randomly precipitated carbon could be observed. On the surface of this sample a carbon-free layer was formed consisting of Ni_2Si. Because of the limited thickness of the thin nickel films following exposure for a few hours at elevated temperature, the complete reaction path could not be determined. More detailed micrographical evidence for the formed interface-like periodic band structure and carbon precipitation will be presented in a future publication using thick nickel foils.

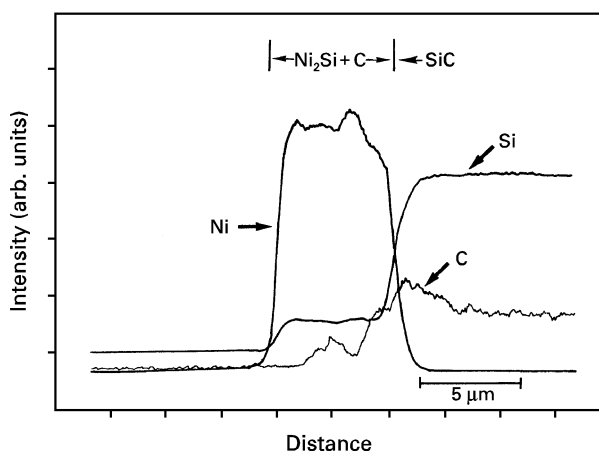

Figure 5 EPMA line scan for nickel, carbon and silicon over the cross-sectional SiC/Ni reaction zone after annealing at 950 °C for 2 h.

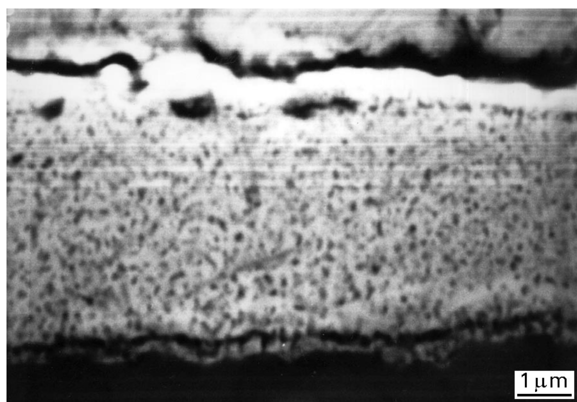

Figure 6 Scanning electron micrograph showing a cross-sectional view of the SiC/Ni reaction zones after annealing at 1050 °C, 2 h.

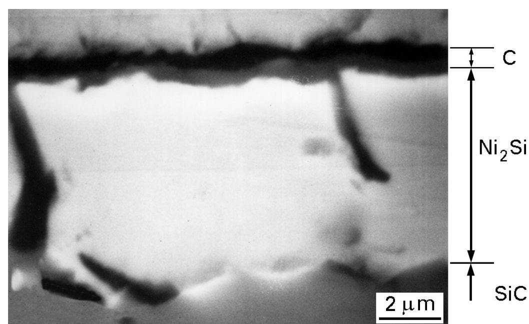

Figure 7 Scanning electron micrograph showing a cross-sectional view of the SiC/Ni reaction zones after annealing at 1250 °C, 2 h.

An increase in temperature to 1250 °C led to graphitization of carbon increasing the intensity of the XRD peaks for graphite. While no carbide was detected in reacted couples at 1250 °C, nickel silicides and graphite were detected by XRD. A cross-sectional scanning electron micrograph (Fig. 7) shows the reaction zones after annealing at 1250 °C for 2 h. The Ni_2Si phase has developed a layer in contact with SiC. Carbon was mainly deposited on the surface of the Ni_2Si phase. At this temperature, a non-periodic structure of carbon precipitations was observed in the Ni_2Si phase. This structure also explains the high X-ray intensity of graphite observed for this sample. The typical phase distribution on the reaction zone at 1250 °C for 2 h can be described as a sequence of $C/Ni_2Si/SiC$.

3.3. Estimation of adhesion strength

Fig. 8 shows an optical micrograph of typical failure mode on scratch channels of the SiC/Ni reaction surface after annealing at 950 °C for 2 h under stylus loads of 31, 32, 33 and 34 N. In order to determine the critical load of the reaction couples, an acoustic signal was emitted in the range 0–200 mV. The procedure for acoustic signal measurements has been previously described [18]. Under low stylus loads of 31 N (channel 1(a) in Fig. 8) and 32 N (channel (b) in Fig. 8) the coatings were smoothed out without any cracking of the coatings on the substrates, and the acoustic signal did not increase at these stages. As the stylus load was increased to 33 N (channel (c) in Fig. 8), the onset of coating loss was accompanied by a sudden increase in the acoustic signal. The load of 33 N at which point the coating was stripped from the substrate with a sudden increase in the acoustic signal was termed the critical load. As the stylus load was further increased, the number of cracks steadily increased

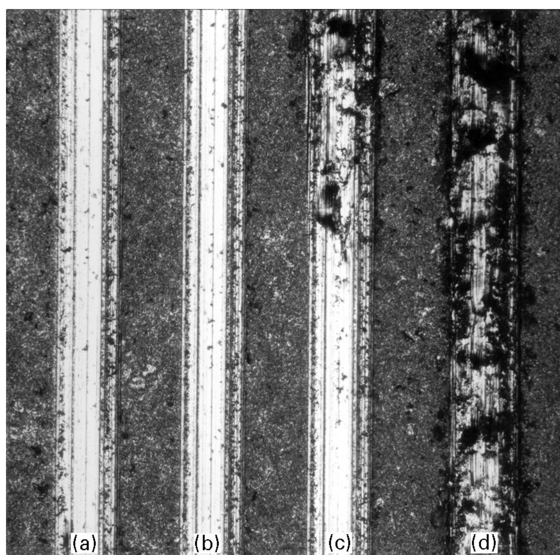

Figure 8 An optical micrograph of the scratch channels of the SiC/Ni reaction surface after annealing at 950 °C for 2 h under various stylus loads: (a) 31 N, (b) 32 N, (c) 33 N and (d) 34 N.

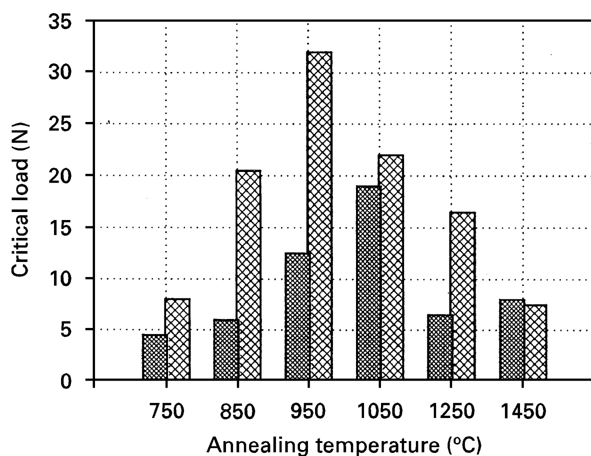

Figure 9 Average critical loads of the SiC/Ni reaction couples compared with SiC/Co for various annealing temperatures. Key: (▩) SiC/Ni and (▩) SiC/Co.

(channel (d) in Fig. 8). The mode of the coating failure appears to vary according to the nature of both the substrate and the coating, the coating thickness and also the method by which the coating is produced. Generally, the critical load increased with increasing coating thickness [27]. In this study the coating thickness was fixed at about 2 μm. Fig. 9 shows the average critical loads of SiC/Ni reaction couples compared with SiC/Co [18] for various annealing temperatures. According to measurements the average critical loads of all the samples were in the range 8–32 N in the temperature range 750–1450 °C. The average critical loads of SiC/Ni were found to be relatively higher compared to that estimated in the SiC/Co system. The relatively higher values of 20–33 N were observed for SiC/Ni couples reacted between 850 and 1050 °C.

4. Discussion

The reaction between a thin nickel film and SiC leads to the formation of nickel silicides and carbon in the form of amorphous precipitates. It is worthwhile discussing the formation of the structure in the reaction zone in terms of the thermodynamics and reaction kinetics. The thermodynamics of the reaction could be described by calculating the Gibb's energy, ΔG_R, for the various reactions within the system (Table I). In Fig. 10 the calculated values of these reactions are plotted as a function of temperature [28]. The result predicts which phases are stable at thermodynamic equilibrium. Nickel is known to react with silicon and form various silicides, Ni_2Si, Ni_3Si_2, NiSi and $NiSi_2$ (reactions 6, 7, 8 and 9 in Fig. 10), because the ΔG values are highly negative. Less negative values are calculated for the corresponding reactions with SiC 2, 3, 4 and 5, because energy is needed for SiC decomposition. Under the present experimental conditions

TABLE I Possible reactions and Gibb's energies, ΔG_T, for the SiC/Ni system. $\Delta G_T = A + BT \log T + CT$

Possible reactions	Temperature functions of Gibb's energy (kJ per g-atom Ni)		
	A	*B*	*C*
$Ni + 1/3SiC \rightarrow 1/3Ni_3C + 1/3Si$	30.793	0.0018	− 0.0103
$Ni + 2SiC \rightarrow NiSi_2 + 2C$	22.990	0.0108	− 0.0454
$Ni + SiC \rightarrow NiSi + C$	− 30.932	0.0054	− 0.0195
$Ni + 2/3SiC \rightarrow 1/3Ni_3Si + 2/3C$	− 38.317	0.0036	− 0.0158
$Ni + 1/2SiC \rightarrow 1/2Ni_2Si + 1/2C$	− 41.800	0.0027	− 0.0119

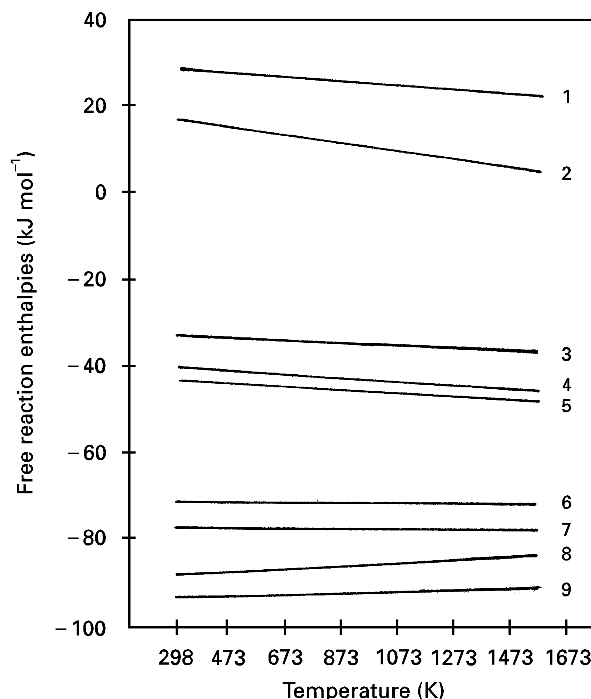

Figure 10 Calculated Gibb's energy for various reactions between SiC and nickel, as well as between silicon and nickel as a function of temperature (based on 1 g-atom Ni). Key: (a) $Ni + 1/3SiC = 1/3Ni_3C + 1/3Si$; (2) $Ni + 2SiC = NiSi_2 + 2C$; (3) $Ni + SiC = NiSi + C$; (4) $Ni + 2/3SiC = 1/3Ni_3Si_2 + 2/3C$; (5) $Ni + 1/2SiC = 1/2Ni_2Si + 1/2C$; (6) $Ni + 1/2Si = 1/2Ni_2Si$; (7) $Ni + 2/3Si = 1/3Ni_3Si_2$; (8) $Ni + Si = NiSi$ and (9) $Ni + 2Si = NiSi_2$.

nickel reacts with SiC and forms the silicides, Ni_3Si_2 and Ni_2Si at the SiC interface. The reason why the NiSi phase was not found despite being expected from the thermodynamic analysis is primarily attributed to the availability of more metal atoms, as compared to Si atoms, in the reaction zone because of a faster consumption rate of the metals [29–32].

In the case of reaction 2, where two moles of SiC should be decomposed per reacted nickel g-atom, ΔG shows slightly positive values. Therefore, $NiSi_2$ could not be formed in this temperature range. In addition, the formation of the carbide Ni_3C (reaction 1) is thermodynamically impossible because this phase is not stable under these conditions. Considering the reaction between SiC and nickel, only the formation of NiSi, Ni_3Si_2 and Ni_2Si shows a negative ΔG value and can be formed by solid state reaction.

Above 750 °C the initially formed Ni_3Si_2 layer was converted to Ni_2Si and additional carbon precipitates were observed within the Ni_2Si phase. According to reported diffusion data [29–32], nickel is the dominant diffused species in nickel silicides. In that way nickel arrives at the SiC interface to react with SiC.

5. Conclusions

The reactivity and morphology of thin sputtered nickel films deposited on SiC were investigated in the temperature range 550–1450 °C. The reaction with the formation of silicides and carbon was first observed above 650 °C. Above 750 °C, as the reaction proceeded, the initially formed Ni_3Si_2 layer was converted in to Ni_2Si and carbon precipitates were observed within this zone. The thin nickel film reacted completely with SiC after annealing at 950 °C for 2 h. The thermodynamically stable Ni_2Si is the only observed silicide in the reaction zone up to 1050 °C. Above 1250 °C, carbon precipitated preferentially on the outer surface of the reaction zone and crystallized as graphite.

The formation of $Ni_2Si + C$ and $Ni_3Si_2 + C$ zones according to the reaction of SiC with thin sputtered nickel films was favoured under the experimental conditions, because the Gibb's energy of both reactions is negative. The formation of $NiSi_2$ was not observed because energy is needed for the decomposition of SiC. The carbide Ni_3C is thermodynamically unstable in this temperature region and the ΔG values of the corresponding reactions with SiC are positive.

The adhesive strength was qualitatively compared in terms of critical load estimated using the scratch test method. According to the measurements the average critical loads for the reaction layers formed at temperatures in the range of 750–1450 °C are between 8 and 33 N. The average critical loads of reaction layers in the SiC/Ni systems are relatively higher than those observed in SiC/Co systems. The relatively higher values of 20 to 33 N for SiC/Ni were measured for samples reacted between 950 and 1050 °C.

References

1. K. D. MÖRGENTHAR, *Tech. Keram.* **2**, edited by J. Kriegermann (Deutsche Keramische Gesellschaft, Köln, 1990) 29.
2. L. M. SHEPPARD, *Ceram. Bull.* **68** (1989) 1624.
3. D. L. MCDALENS, T. T. SERAFINI and J. A. DICARLO, *J. Mater. Energy System* **8** (1986) 80.
4. G. L. HARRIS, M. G. SPENCER and C. Y.-W. YANG, "Amorphous and crystalline silicon carbide III" (Springer-Verlag, Berlin 1992).
5. R. J. TREW, J. B. YAN and P. M. MOCK, *Proc. IEEE* **79** (1991) 598.
6. R. F.DAVIS, G. KELNER, M. SHUR, W. PALMOUR and J. A. EDMOND, *ibid.* **80** (1991) 667.
7. M. G. NICHOLAS, *Mater. Sci. Res.* **21** (1986) 349.
8. D. J. LARKIN, L. V. INTERRANTE and A. BOSE, *J. Mater. Res.* **5** (1990) 2706.
9. R. E. LOEHMAN, *Ceram. Bull.* **68** (1989) 891.
10. R. C. J. SCHIEPERS, F. J. J. VAN LOO and G. D. WITH, *J. Amer. Ceram. Soc.* **71** (1988) C-284.
11. M. BACKHAUS-RICOULT, *Ber. Bunsenges. Phys. Chem.* **93** (1989) 1277.
12. T. C. CHOU, A. JOSHI and J. WADSWORTH, *J. Mater. Res.* **6** (1991) 796.
13. P. NIKOLOPOULOS, S. AGATHOPOULOS, G. N. ANGELOPOULOS, A. NAOUMIDIS and H. GRÜBMEIER, *J. Mat. Sci.* **27** (1992) 139.
14. E. GYARMATI, W. KESTERNICH and R. FÖRTHMANN, cfi/Ber. DKG 66 (1989) 292.
15. D. L. YANEY and A. JOSHI, *J. Mater. Res.* **5** (1990) 2197.
16. T. C. CHOU and T. G. NIEH, *ibid.* **5** (1990) 1985.
17. V. M. BERMUDES and R. KAPLAN, *ibid.* **5** (1990) 2882.
18. C. S. LIM, H. NICKEL, A. NAOUMIDIS and E. GYARMATI, *J. Mater. Sci.* **30** (1995) 3874.
19. *Idem, ibid.* **31** (1995) 4241.
20. D. FATHY, O. W. HOLLAND, J. NARAYAN and B. R. APPLETON, *Nucl. Instr. Meth. Phys. Res.* **B7** (1985) 571.
21. H. HÖCHST, W. NILES, G. W. ZAJAC, T. H. FLEISCH, B. C. JOHNSON and J. M. MEESE, *J. Vac. Sci. Technol.* **B6** (1988) 1320.
22. W. F. J. SLIJKERMAN, A. E. M. J. FISCHER, J. F. VAN DER VEEN, I. OHDOMARI, S. YOSHIDA and S. MISAWA, *J. Appl. Phys.* **66** (1989) 666.
23. I. OHDOMARI, S. SHA, H. AOCHI, T. CHIKYOW and S. SUZUKI, *ibid.* **62** (1987) 3747.
24. C. S. PAI, C. M. HANSON and S. S. LAU, *ibid.* **57** (1985) 618.
25. J. NARAYAN, D. FATHY, O. W. HOLLAND, B. R. APPLETON and R. F. DAVIS, *ibid.* **56** (1984) 1557.
26. M. OHRING, "The materials science of thin films" (Academic Press, London, 1992) p. 113.
27. A. J. PERRY, *Thin Solid Films* **78** (1981) 77.
28. O. KUBASCHEWSKI and C. B. ALCOCK, "Metallurgical thermochemistry", 5th Edn. (Pergamon Press, Oxford, 1983) p. 280.
29. R. M. WALSER and R. W. BÉNE, *Appl. Phys. Lett.* **28** (1976) 624.
30. C. D. LIEN, M. A. NICLOET and S. S. LAU, *Thin Solid Films* **143** (1986) 63.
31. K. N. TU, W. K. CHU and J. W. MAYER, *ibid.* **25** (1975) 403.
32. F. D'HEURLE, C. S. PETERSON, J. E. E. BAGLIN, S. J. LA PLACA and C. Y. WONG, *J. Appl. Phys.* **55** (1984) 4208.

Received 19 April 1996
and accepted 20 April 1997